Landslide susceptibility maps in the rock slopes of the Ventotene Island (Latium, Italy)

I. Caso [1], R. D'Angelo [1], B. Palma [1], M. Parise [2], A. Ruocco [1]

[1] IdroGeo Srl, Vico Equense, Italy
[2] CNR-IRPI, Bari, Italy (m.parise@ba.irpi.cnr.it)

Abstract
The paper illustrates an application of the Matheson test, implemented in GIS environment, to the cliffs of the volcanic island of Ventotene (Pontine Archipelago, Italy). Starting from detailed field study and geo-structural analysis, four failure mechanisms were considered for the analysis (planar sliding, wedge failure, flexural toppling, and block toppling), and a susceptibility map was produced as a cartographic representation of the rock failures affecting the cliffs around the island.

Keywords: susceptibility, landslide, volcanic island, Ventotene

1. Introduction

Rock slopes are typically affected by different types of failures, mostly dependent upon the number and frequency of discontinuity families in the rock mass, combined to the slope main direction. In case of wide areas, a punctual approach, consisting in detailed analysis site per site, is not feasible due to time and money constraints. It is therefore necessary to define automated procedures which, starting from field data collected in sample areas, might represent the likely conditions of instability. In this paper, moving from the above considerations, we apply the test of Matheson (1983) to the cliffs of the volcanic island of Ventotene (Pontine Archipelago, Latium, Italy), intensely affected by occurrence of rock failures (Fig. 1.1), and present the related susceptibility map of the island.

2. Geological and morphological setting

The Pontine Archipelago consists of several islands located at about 50 km from the Tyrrhenian coastline, that can be divided into two groups: the western islands (Palmarola, Ponza, Zannone and the Botte rock), and the eastern islands (Ventotene and S. Stefano). Ventotene (3 km-long, maximum width 800 m) represents the exposed part of a volcano with base of about 300 km^2 and elevation of over 700 m (Perrotta et al., 1996). The eruptive center was located 2-3 km W of

Ventotene (Metrich et al., 1988), as indicated by the volcanic products cropping out on the island, dipping to the NE (Bergomi et al., 1969). The original volcanic building was a strato-volcano, built through effusive and explosive eruptions during the last 800.000 years (Perrotta et al., 1996), with at least 27 eruptive phases, and intervening dormant periods documented by the presence of paleosoils.
The island presents a tuff highplain slightly dipping toward NE, bounded by active cliffs from 130 m (S sector) to 10 m (N sector) high. The highplain is covered by aeolian sediments of pyroclastic origin, and its monotony is broken by small valleys with flat thalweg, typically controlled by the main discontinuties in the tuff.
The deposits can be correlated, for both age (<1 Ma, after Metrich et al., 1988) and composition, to the potassic association of the Roman Comagmatic Province. They may be grouped in 4 lithological units (Fig. 2.1): flows; loose to weakly welded, locally pedogenized, pyroclastic deposits; tuffs (soft rocks); aeolian deposits.
The lava flows have to be referred to trachi-basalt flows deposited in submarine environment, with interbedded red scoria layers. They represent the base of the volcanic sequence and crop out widely in the southern sector of the island.
The loose to weakly welded pyroclastic deposits mantle the flows, forming the central part of the island and diffusely cropping out in the middle to low portions of the cliffs. They consist of alternating levels of ashes, pumice, lithics and paleosoils emplaced by pyroclastic flows (surge) and falls. The pumice and scoria levels can be considered a loose rock. At the top the succession is characterized by a stratigraphic marker, a level of some 50 cm of white pumice.
In the central-southern sector of the island, above the flows, two different pyroclastic horizons can be recognized: 1) alternating white pumice by fall, paleosoils and loose to pseudo-cemented ash layers with undulated structure, and 2) highly compacted trachi-basaltic scoria, intercalated to thin lava flows.
The tuffs (alkali-trachitic pyroclastic flows, with structure from massive to undulated) crop out mostly in the north, representing the highest stratigraphic element. The ash matrix includes lithics and juveniles (sub-rounded scoria and grey pumice). The post-depositional zeolitization processes transformed the deposit in a soft rock crossed by several discontinuity systems, in addition to the bedding.
A 3 paleosoils unit is eventually found between the tuff and pyroclastic deposits.

3. The test of Matheson, and its implementation in GIS

The method by Matheson (1983) is a criterion of block stability that, based upon a geomorphological – geomechanical approach, allows to evaluate the susceptibility of a slope to develop instabilities. Differently than the general stability methods that calculate the quantitative ratio between the stabilizing and destabilizing forces in a slope subjected to translational-rotational phenomena, the Matheson method allows to perform a kinematic analysis of the blocks left isolated by the discontinuities, without taking into account the forces. It is based on representations in emispheric projection of the discontinuity data, and correlates the preparatory conditions of rock failures by graphically delimiting a critical area. If the poles representing a discontinuity family fall within this area, the test is positive with regard to the considered kinematic typology, and the blocks bounded by this family are potentially unstable. The rock mass is schematically analyzed by representing the following parameters, in the hypothesis that the discontinuities are plane and infinitely persistent: i) dip direction and dip of the slope; ii) dip direction and dip of the discontinuities; iii) friction angle of the rock mass.

It is necessary to have a sufficiently high number of data to represent a reliable sample of the population of discontinuities in the rock mass. The method takes into account the real variability of the rock mass, since it considers in situ measurements. The criterion of delimitation of the critical area changes in function of the type of instability. Four different failure mechanisms are considered: i) planar sliding; ii) wedge failure; iii) flexural toppling; iv) block toppling.

Development of Geographic Information Systems (GIS) has allowed to perform totally automated operations of data superimposition and integration, thus permitting a georeferenced mapping and managing the results in forms of a database. The informative layers are the base maps, distinguished into two different groups: (i) *cell grids* (raster), 1.1 x 1.1 meters, where at each elementary cell a value is assigned for each considered factor: this base is used to build the informative layer containing the data of dip direction of the slopes obtained from GIS processing of the topographic map; (ii) *terrain unit*, bounded by lines that reflect the geomorphological and/or geological variables in the territory. Identification of the slopes (cliffs) where the rock failures may potentially occur corresponds to this unit. For this boundary the dip of the slope is sub-vertical (85÷90°).

The friction angle of the rock mass is assumed constant and was estimated 35° from Beniawski characterization. Dip direction and dip of discontinuities were measured in the field, by performing geo-structural surveys in 5 sample areas (fig. 1.1), and graphically portraying the data in polar equiareal projection. Three main discontinuity families (K1: 69/89, K2: 156/90, K3: 26/89) have been identified, in addition to bedding (S_b: 70/12). Given the volcano-tectonic framework of the area, and the agreement of the data with further additional measurements, the recognized geo-structural setting has been then extrapolated to the rest of the island.

The conditions to verify the tests of Matheson are well suited to the implementation of the method in a computational routine, that performs cyclic and conditional operations of Map Algebra. For each failure mechanism the routine controls the triggering conditions and provides a map in boolean language of the test outcomes over the whole base map. Taking, as an example, the planar sliding, the algorithm performs two tests for each cell: the first checks the dip input data, founding the cell were the dip of the discontinuity families is lower than the dip of the slope but greater than the friction angle; the second routine verifies the dip direction data, founding the cells where the angle formed by discontinuities and slopes does not overcome 20°. By superimposing sequentially the outcomes of the two routines for each single discontinuity family, a series of four thematic maps is produced, each containing information on the susceptibility for the analyzed mechanism.

4. Susceptibility map

The Matheson tests, implemented in GIS environment, have been applied to the island of Ventotene, starting from the geo-structural data measured in the field. Table 4.1 summarizes the square area interested by each failure mechanism. The outcomes are expressed also in percentage, in reference to the area occupied by the cliffs. Based upon these results, a zonation map was produced by summing the number of mechanisms potentially occurring and ranking in four classes the susceptibility. The susceptibility map (Fig. 4.1) shows that most of the island is severely affected by possibility of failures; the highest classes are concentrated in the western and southern sector, but also the rest of the cliffs are not immune to instability, as recently demonstrated by the tragic event occurred at Cala Rossano on April 20, 2010, that caused two fatalities.
The main outcome of the implementation of the Matheson tests in GIS environment is represented, once the input data are available and sufficiently representative of the whole study area, by the rapid assessment of the failure mechanisms and the possibility of an easy management of robust datasets, even for very large areas. In the specific case of the Ventotene island, characterized for most of its length by high cliffs, the applied methodology allowed to identify at each site the instability conditions, including the most likely mechanism of failure. This latter point, in particular, is extremely useful to design the most proper stabilization works, aimed at mitigating the landslide risk.

References

Bellucci F., Lirer L., Rolandi G., 1999. *Geological map of Ponza, Ventotene and Santo Stefano islands.* Dip. Geofisica e Vulcanologia, Univ. Napoli Federico II.
Bergomi C., Catenacci V., Cestari G., Manfredini M., Manganelli V., 1969. *Note illustrative del F. 171 Gaeta e vulcano di Roccamonfina.* Serv. Geol. It., 140 pp.
Matheson G.D., 1983. *Rock stability assessment in preliminary investigations. Graphical methods*. Department of the Environment, Department of Transport and Road Research Laboratory Report LR 1039.
Metrich N., Santacroce R. and Savelli C., 1988. *Ventotene, a potassic Quaternary volcano in central Tyrrhenian Sea.* Rend. Soc. It. Mineral. Petrol. 43: 1195-1213.
Perrotta A., Scarpati C., Giacomelli L., Capozzi A., 1996. *Proximal depositional facies from a caldera forming eruption: The Parata Grande Tuff at Ventotene Island (Italy)*. Journal of Volcanology and Geothermal Research 71: 207-228.

Table 4.1 – Surfaces affected by instabilities in the Ventotene Island. K1, K2 and K3 are the main families of discontinuities, S_b is the bedding.

Fig. 1.1 – Examples of rock failures at Ventotene: a) 2012 planar sliding in the NW sector (Cala di Parata Grande); b) landslide body detached from a cliff N from Parata Grande; c) April 20, 2010, event at Cala Rossano (two fatalities); d) artificial caves of the old roman aqueduct also contribute to slope instability.

Fig. 2.1 - Geolithological map (after Bellucci et al., 1999): 1) Loose aeolian deposits, consisting of reworked pyroclastic materials. 2) Tuff. 3) Loose and weakly welded pyroclastic deposits, locally turning in soil. 4) Lava flows.

Fig. 4.1 - Susceptibility map of Ventotene Island.

Planar sliding	**K1**		**K2**		**K3**	
area (m^2)/%	7.137	6,1	22.427	19,0	14.798	12,6
Flexural toppling	**K1**		**K2**		**K3**	
area (m^2)/%	1.786	1,5	26.952	22,9	3.493	3,0
Wedge failure	**K1, K2**		**K1, K3**		**K2, K3**	
area (m^2)/%	46.563	39,5	56.747	48,2	55.632	47,2
Block toppling	**S_b, K1, K2**		**S_b, K1, K3**		**S_b, K2, K3**	
area (m^2)/%	0	0,0	7.134	6,1	0	0,0

Table 4.1

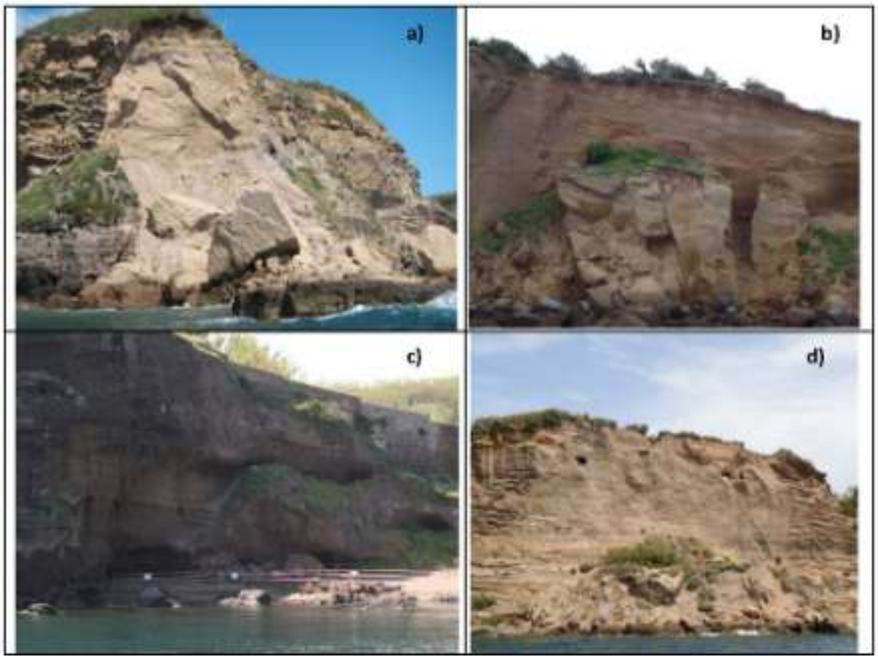

Fig.1.1

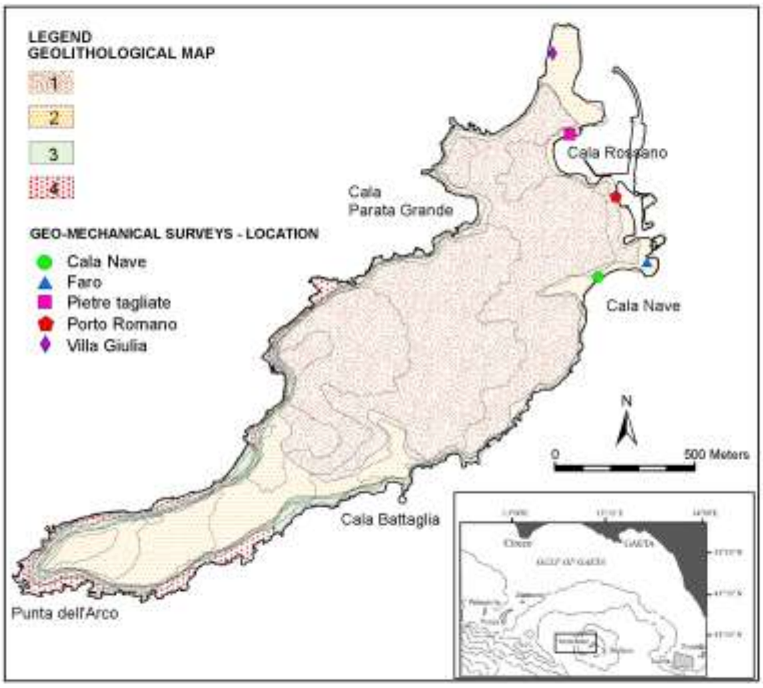
LEGEND
GEOLITHOLOGICAL MAP
1
2
3
4
GEO-MECHANICAL SURVEYS - LOCATION
Cala Nave
Faro
Pietre tagliate
Porto Romano
Villa Giulia
Cala Rossano
Cala
Parata Grande
Cala Nave
N
0
500 Meters
Cala Battaglia
Punta dell'Arco

Fig. 2.1

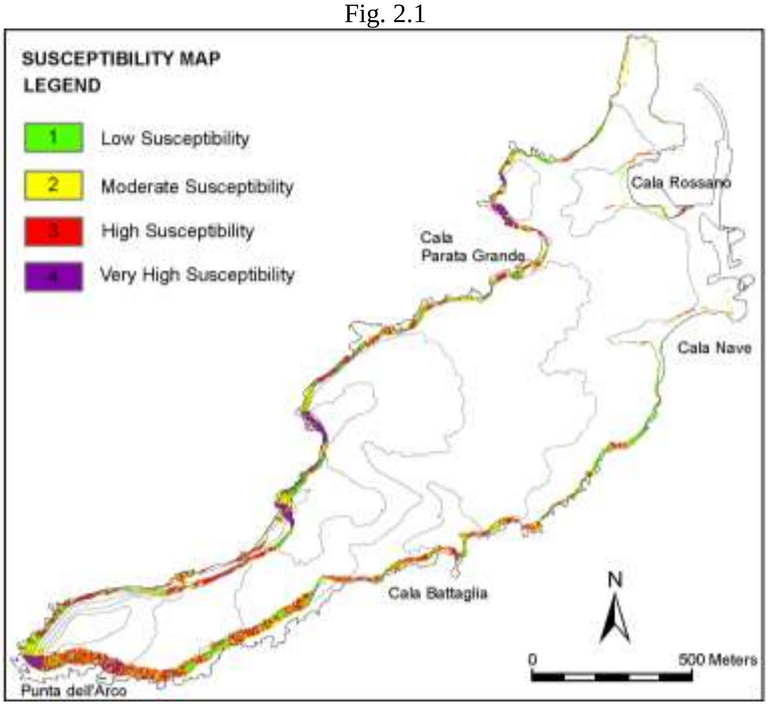
SUSCEPTIBILITY MAP
LEGEND
1 Low Susceptibility
2 Moderate Susceptibility
3 High Susceptibility
4 Very High Susceptibility
Cala Rossano
Cala
Parata Grande
Cala Nave
Cala Battaglia
N
0
500 Meters
Punta dell'Arco

Fig. 4.1